Thermotropic Behavior of Dimyristoylphosphatidylglycerol and Its Interaction with Cytochrome c[†]

Thomas Heimburg[‡] and Rodney L. Biltonen[*]

Departments of Biochemistry and Pharmacology, University of Virginia Health Sciences Center, Charlottesville, Virginia 22908

Received December 2, 1993; Revised Manuscript Received May 27, 1994[®]

ABSTRACT: The thermotropic behavior of dimyristoylphosphatidylglycerol (DMPG) in the absence and presence of cytochrome c under low-salt conditions has been investigated using differential scanning calorimetry (DSC), ^{31}P nuclear magnetic resonance (^{31}P NMR), electron spin resonance (ESR), viscosity, light scattering, and electron microscopy. In the absence of protein, the lipid undergoes a sequence of transitions over the temperature range of 7–40 °C. ESR studies demonstrate increased acyl chain mobility associated with these transitions. ^{31}P NMR indicates that the lipid, in the absence of protein, retains a lamellar structure throughout the temperature range investigated. At high lipid concentration the DSC curves exhibit a pronounced maximum in the excess heat capacity (C_p) function at about 23 °C with a shoulder on the high-temperature side. As the lipid concentration is reduced to 10 mM, the C_p curves broaden, retaining a sharp maximum at about 20 °C and a broader transition with a maximum at 27 °C. The overall enthalpy change of 6 kcal/mol is independent of lipid concentration. Most interestingly, the lipid dispersion becomes highly viscous and optically isotropic in the main transition range (20–28 °C), suggesting long-range order even at lipid concentrations as low as 10 mM. The existence of long-range order is confirmed by negative stain electron microscopy. The heat capacity curve in the presence of protein is broad, with a single C_p maximum and an overall enthalpy change of 1.7 kcal/mol. Similarly, the temperature dependence of the ESR spectra shows none of the detail observed in the absence of the protein. Of specific interest is that partially saturating amounts of protein prevented the large increase in the viscosity of the dispersion in the main transition range. This result suggested that the protein prevented development of long-range order. However, under saturating conditions the viscosity of the protein–lipid complex increased with increasing temperature even beyond the transition range. This increase does not appear to be the result of formation of an extended lipid structure but is the result, according to electron microscopic evaluation, of aggregation of small protein-containing lipid vesicles. The ^{31}P NMR spectra of the lipid in the presence of protein are isotropic, consistent with the formation of highly curved particles. Calorimetric titration studies of the binding of cytochrome c to DMPG indicate that protein binding is coupled cooperatively to changes in the state of the lipid. The binding data were analyzed in terms of a model in which the protein binds differentially to two different states of the lipid. This analysis yielded estimates of the binding affinity on the order of 10^6 L/mol and a stoichiometry of about 9:1, lipid to protein. The binding does not appear to involve any change in the degree of protonation, and the protein-induced change in lipid structure likely makes a significant contribution to the measured enthalpy change.

Lipid aggregates of various types form spontaneously upon hydration. The predominant organization is in the form of bilayers. Lipids can also assemble into other structures such as micelles, rod-like hexagonal phases, and cubic phases. It has been suggested that the latter two forms may be involved in fusion, fission, and transport properties of the cell membrane (Lindblom & Rilfors, 1989; Mariani et al., 1988). Most lipids show a broad mixing gap between water and fully hydrated lipid (i.e., a bulk water phase exists over a broad range of lipid concentrations), although this is not necessarily true for all lipids. For example, zwitterionic phospholipids are fully hydrated at a molar ratio of about 1:20, lipid:water (Seddon et al., 1984); further addition of water results in no further change of the structural organization of the lipids. On the other hand, most detergent systems form phases that are concentration dependent over the full range of water con-

centration. Which phase exists is dependent on the lipid composition, the temperature, the ionic strength of the aqueous phase, and last but not least, the nature of membrane-associated proteins.

The characteristics of a temperature-dependent structural transition of a lipid system can be altered greatly by a protein, if the protein thermodynamically prefers one lipid state over another (Sperotto & Mouritsen, 1991). Conversely, the state of the lipid can influence the binding properties of the protein if such a preference exists. Furthermore, if a membrane-bound protein exists in more than one state, the equilibrium poise between forms will be determined, in large part, by the state of the lipid. The coupling between lipid transitions and protein conformational changes can be well described by rigorous thermodynamic relationships if the states involved are defined and the microscopic thermodynamic constants are known. Unfortunately, these latter two conditions are not generally satisfied for any experimental membrane system. In spite of this, many mechanisms of activation and regulation of the biological function of membrane–protein systems are based on such a concept. There are a few cases, however, where changes in the lipid state have been shown to alter the

structure or activity of bound proteins. These include phospholipase A_2 (Bell & Biltonen, 1989; Jain & Berg, 1989), protein kinase C (Epand & Lester, 1990), β-dehydroxybutyrate dehydrogenase (Cortese & Fleischer, 1987), and cytochrome c (Hildebrandt et al., 1990; Heimburg et al., 1991). In some cases, protein association can induce morphological changes in the lipid matrix. For example, cytochrome c binding can induce an H_{II} phase in cardiolipin (De Kruijff & Cullis, 1980) and cubic phases with monoolein (Mariani et al., 1988).

Cytochrome c is a particularly interesting case. Its interaction with charged lipid surfaces has been studied previously by resonance Raman spectroscopy (Hildebrandt & Stockburger, 1989a,b; Hildebrandt et al., 1990; Heimburg et al., 1991). In all cases, coupling between binding and the distribution of two distinct protein states with different redox potentials could be demonstrated. Further evidence for an influence of protein binding on the structure of dioleoylphosphatidylglycerol (DOPG)[1] membranes has been obtained by phosphorus nuclear magnetic resonance (^{31}P NMR) (Heimburg et al., 1991). At 20 °C a phosphorus spectrum typical of a liquid crystalline lamellar phase is observed. As cytochrome c is added to the lipid, an isotropic ^{31}P NMR component becomes evident, an indication that the lipid–H_2O system changes its three-dimensional organization. It is thus clear that this protein can exist in at least two distinct states on a lipid surface and that its binding can induce a structural change in the lipid. In order to obtain information regarding the nature of the thermodynamic coupling of these structural changes, we initiated a study directed toward understanding the relationship between the thermotropic behavior of the lipid and the binding of cytochrome c to the lipid surface.

Dimyristoylphosphatidylglycerol (DMPG) was chosen as the charged lipid because it has been used previously in structural and thermodynamic studies of cytochrome c–lipid interactions. However, the thermotropic behavior of DMPG has not been well described, and evidence for a quite unusual behavior of this lipid has been published (Gershfeld et al., 1986; Gershfeld, 1989). Therefore, we first report on the lipid concentration and protein concentration dependence of the physical properties of DMPG dispersions obtained using differential scanning calorimetry (DSC), viscometry, light scattering, electron microscopy, electron spin resonance (ESR), and ^{31}P NMR. These results demonstrate that at low salt the temperature-dependent, polymorphic structure of DMPG is concentration dependent even at lipid to water ratios of $1:10^5$ and influenced strongly by the presence of protein. The thermodynamics of cytochrome c binding to DMPG, obtained by titration calorimetry, are then interpreted within the framework of a model which couples protein binding to the temperature-dependent changes in the polymorphic structure of DMPG.

MATERIALS AND METHODS

Materials. The sodium salt of dimyristoylphosphatidylglycerol (DMPG) (Avanti Polar Lipids, Birmingham, AL) was used without further purification. Purity was checked by TLC. The lipid was dried from a chloroform solution, lyophilized, dispersed in buffer (2 mM TRIS, HEPES, or phosphate and 1 mM EDTA, pH 7.5), and vortexed above the phase transition temperature (above 30 °C). Except for the DSC experiments at the highest lipid concentrations, the pH of the dispersion was adjusted to pH 7.5. At room temperature a clear, jelly-like structure formed. At temperatures below 20 and above 30 °C, the dispersion appeared to be of low viscosity and the optical appearance was milky. Cytochrome c (Sigma, horse heart type III oxidized form) was used without further purification.

C-14 spin-labeled fatty acid (14-SASL) was synthesized and used to acylate lysophosphatidylcholine to yield the corresponding spin-labeled diacylphosphatidylcholine (14-PCSL) following the procedure of Marsh and Watts (1982). The C-14-labeled phosphatidylglycerol (14-PGSL) was synthesized from 14-PCSL, using head group exchange catalyzed by phospholipase D, according to Comfurius and Zwaal (1977).
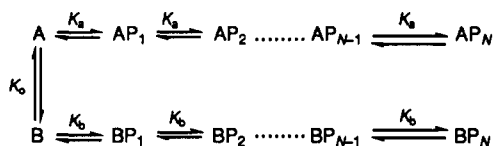
Differential Scanning Calorimetry. Heat capacity measurements of lipid and lipid–protein dispersions were performed on a Hart Scientific differential scanning calorimeter (DSC) at scan rates of 20 °C/h and on a high-sensitivity differential scanning calorimeter constructed in this laboratory (Suurkuusk et al., 1976) at several scan rates. The experimental data were corrected for the time response of the calorimeter. The pH of the dispersions varied generally from pH 7.5 to 7.8. For small-volume samples, pH adjustment to pH 7.5 was not always possible. All scans were performed with phosphate-buffered dispersions. Since the enthalpy of ionization of phosphate is very small, the pK_a of the buffer and, hence, the pH will vary little with temperature. Furthermore, the pK_a of DMPG should be <6 at these ionic conditions, and thus, small variations in pH should have little effect on the charge state of the lipid.

Isothermal Titration Calorimetry. Enthalpy titrations were performed with a Microcal MC-2 microcalorimeter with an Omega reaction cell. A detailed description of this calorimeter is given in Wiseman et al. (1989). The protein was added to the lipid dispersion with a rotating syringe (300 rpm) that also stirs the solution in the cell. Lipid concentrations were 0.5 mg of DMPG/cell volume (0.536 mM) with 20 mg/mL cytochrome c in the syringe (1.61 mM). The heat associated with injection of the cytochrome c solution into the lipid dispersion was recorded in each experiment to obtain the enthalpy binding isotherm. Each of the 10 or 11 injections of the protein solution was added continuously during a 30-s period. Prior to the experiment, the lipid and protein solutions were adjusted to pH 7.5 with an accuracy of 0.01 to minimize any heat of mixing of the buffered solutions. The heat of dilution of the protein solution was subtracted from the measured heat of mixing to obtain the enthalpy binding isotherm. The reproducibility of the heat of a binding isotherm was ±0.2 kcal/mol of lipid.

Analysis of Calorimetric Binding Data. The model we have chosen to analyze the calorimetric binding data is based upon two sets of crucial observations which will be described in the Results section. First, the calorimetric data exhibit cooperative and/or biphasic behavior (Figures 9 and 11). Second, the DSC (Figure 2), viscosity (Figure 3b), ESR (Figures 5 and 6), and, especially, NMR (Figure 7) data show clearly that the protein induces a change in the structural organization of the lipid. It thus follows that a model coupling protein binding to a lipid structural change must be invoked.

---

[1] Abbreviations: 14-SASL, 14-(4,4-dimethyloxazolidine-*N*-oxyl)-stearic acid; 14-PCSL, 1-acyl-2-[14-(4,4-dimethyloxazolidine-*N*-oxyl)-stearoyl]phosphocholine; 14-PGSL, 1-acyl-2-[14-(4,4-dimethyloxazolidine-*N*-oxyl)stearoyl]phosphoglycerol; DMPG, 1,2-dimyristoyl-*sn*-glycero-3-phosphoglycerol; DOPG, 1,2-dioleoyl-*sn*-glycero-3-phosphoglycerol; ^{31}P NMR, phosphorus-31 nuclear magnetic resonance; ESR, electron spin resonance; DSC, differential scanning calorimetry; TRIS, tris(hydroxymethyl)aminomethane; HEPES, 4-(2-hydroxyethyl)-1-piperazineethanesulfonic acid; EDTA, ethylenediaminetetraacetic acid; PLA2, phospholipase A_2; PKC, protein kinase C; t_m, melting temperature; $\Delta T_{1/2}$, width at half-height of the C_p curve; C_p, excess heat capacity at constant pressure.

The simplest form of such a model is one in which the lipid can exist as an equilibrium mixture of two forms, both of which have the same number (>1) of identical and independent binding sites. This model is described by the following equilibrium reaction scheme.

$$A \rightleftharpoons^{K_a} AP_1 \rightleftharpoons^{K_a} AP_2 \dots\dots AP_{N-1} \rightleftharpoons^{K_a} AP_N$$
$$K_o \updownarrow$$
$$B \rightleftharpoons^{K_b} BP_1 \rightleftharpoons^{K_b} BP_2 \dots\dots BP_{N-1} \rightleftharpoons^{K_b} BP_N$$

where A and B represent the two hypothetical forms of the cooperative unit of the lipid. We define cooperative unit as that number of lipids representing N independent protein binding sites which undergo the A $\rightarrow$ B transition in an all-or-none manner. AP_i and BP_i represent the two forms of the lipid, each having i protein molecules bound. K_o is the equilibrium constant for the lipid structural change in the absence of protein; $K_o = [B]/[A]$. K_a and K_b are the site binding constants for forms A and B of the lipid. In order to observe significant positive cooperative binding and a protein-induced structural change, the following thermodynamic criteria must be met: $K_o \ll 1$ and $K_B > K_A$ (or conversely, $K_o \gg 1$ and $K_a > K_b$). Furthermore, the decrease in the total Gibbs energy change for binding achieved by changing lipid structure must be significantly more favorable than the Gibbs energy change associated with the lipid structural change in the absence of protein binding. That is,

$$-\delta\Delta G^\circ = NRT \ln(K_b/K_a) \gg -RT \ln K_o = \Delta G_o^\circ$$

In addition to these four parameters (N, K_o, K_a, and K_b), three additional parameters are required to define the enthalpy binding isotherm. These are ΔH_o°, the enthalpy change associated with the lipid transition A $\rightarrow$ B, and ΔH_a and ΔH_b, the enthalpy changes associated with protein binding to form A and form B, respectively. ΔH_o° is defined per mole of cooperative unit where ΔH_a and ΔH_b are per mole of site (or protein bound). Insofar as $\Delta H_o^\circ + N\Delta H_b$ is the total enthalpy change for the transition of a cooperative unit from state A with zero protein bound to state B with N proteins bound, ΔH_o° and ΔH_b are strongly coupled statistically. We therefore have assumed that $\Delta H_o^\circ = 0$. It then follows that the measured enthalpy change (per mole of cooperative unit) is

$$\Delta H = \frac{\sum_{j=1}^{N}(\Delta H_a K_a^j + \Delta H_b K_o K_b^j) j \Omega_j [P]^j}{\sum_{j=0}^{N}(K_a^j + K_o K_b^j) \Omega_j [P]^j}$$

where $\Omega_j = N!/j!(N-j)!$ and $[P]$ = free protein concentration. The free protein concentration is given by

$$[P] = [P_t] - \frac{\sum_{j=1}^{N}(K_a^j + K_o K_b^j) j \Omega_j [P]^j [L_t]/M}{\sum_{j=0}^{N}(K_a^j + K_o K_b^j) \Omega_j [P]^j}$$

where $[P_t]$ and $[L_t]$ are the total protein and lipid concentrations and M is the number of lipids per binding site. For a given N_1, K_a, K_b, and K_o, $[P]$ can be calculated. Assuming $N = 25$, enthalpy binding isotherms were then simulated for

various values of M, K_o, K_a, K_B, ΔH_a, and ΔH_B until good correspondence between the calculated and experimental results was achieved. We realize that this model is an oversimplification and the parameters reported in Table 1 are probably not unique. Nevertheless, the calculated parameters provide a basis for a more quantitative description and discussion of the experimental results. The binding model we have used is analogous to ligand binding to a protein which can exist in two conformational states such as the Monod–Wyman–Changeux model for the binding of oxygen to hemoglobin (Monod et al., 1965). A complete description of linked function analysis is given in Wyman and Gill (1991.)

Electron Spin Resonance (ESR) Spectroscopy. ESR spectra were recorded on a 9-GHz spectrometer (E-line; Varian Associates, Instrument Division, Palo Alto, CA) equipped with a nitrogen gas flow temperature regulator. Lipid dispersions and complexes of lipid and protein were contained in sealed 1-mm-i.d. 100-glass capillaries that were placed inside a 4-mm-diameter quartz ESR tube that contained silicone oil for thermal stability. The temperature was controlled with a fine-wire thermocouple positioned in the silicone oil.

^{31}P Nuclear Magnetic Resonance Spectroscopy. Proton dipolar decoupled ^{31}P NMR spectra were recorded at a frequency of 121.49 MHz on a Bruker MSL-300 spectrometer (Bruker Analytische Messtechnik GmbH, Karlsruhe, Germany) using an 11-μs rf pulse. The decoupling power was approximately 8 W. Temperature was controlled via nitrogen gas flow.

Viscosity and Light-Scattering Measurements. The relative viscosities of the lipid dispersions were obtained using a Cannon K215 viscometer in which the flow times of 13 mM lipid dispersions in the presence or the absence of protein were measured. Ninety degree light scattering was measured with an SLM 8000 fluorimeter (SLM Instruments, Inc.) at a wavelength of 280 nm. In all isothermal experiments, the temperature was maintained to $\pm$0.1 °C with an external water bath.

Electron Microscopy. Negative stain electron microscopy was performed as described in Gonias et al. (1988) except that no glutaraldehyde fixation was employed.

RESULTS

Differential Scanning Calorimetry. The apparent excess heat capacity functions of several DMPG dispersions are shown in Figure 1. At lipid concentrations above 150 mM, the heat capacity curves are typical of those of many other lipid dispersions. Transitions centered at 12 and about 23 °C were observed. These transition temperatures for DMPG are in agreement with previous reports (Gershfeld, 1986; Surewicz et al., 1987). The calorimetric scans of DMPG change with concentration down to the lowest recorded concentration (10 mM), although the total ΔH was found to be independent of concentration. In all cases, the transitions were found to be reversible. As the concentration is reduced, the lowest temperature transition sharpens and moves to about 15 °C, whereas the major transition develops into a sharp C_p peak at about 20 °C with a broad, complex heat capacity profile extending from 20 to 28 °C.

At 10 mM DMPG, the time dependence of the thermotropic lipid transition was investigated using scan rates from 1 to 20 °C/h (data not shown.) The lowest temperature transition ($t_m \sim 15°$) moves to higher temperatures at higher scan rates, indicating it is relatively slow. The low-temperature end of the main transition (20–28 °C) exhibits a sharp peak whose width at half-height ($\Delta T_{1/2}$) is scan rate dependent. The peak
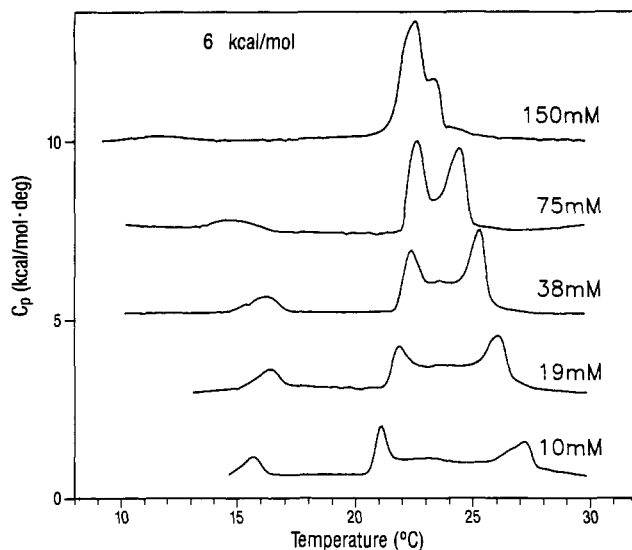
FIGURE 1: Time-response-corrected heat capacity curves of DMPG dispersions at 150, 75, 38, 19, and 10 mM obtained at a scan rate of 20°/h at pH ~ 7.5, in 2 mM phosphate buffer and 1 mM EDTA. Scans were obtained with a Hart Scientific differential scanning calorimeter.
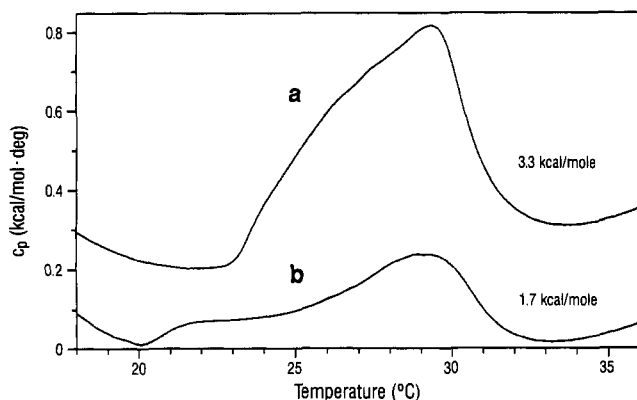

FIGURE 2: Time-response-corrected heat capacity curves of 45 mM DMPG dispersions in the presence of (a) 2.25 and (b) 4.5 mM cytochrome c. Scans were obtained with a Hart Scientific differential scanning calorimeter. The data have not been baseline corrected.

becomes narrower and more pronounced at slower scan rates ($\Delta T_{1/2}$ = 0.3 °C at a scan rate of 1 °C/h), although the position and the integrated enthalpy change remain constant (0.38 ± 0.17 kcal/mol of lipid). The shape of the remainder of this transition is not scan rate dependent. The majority of the heat associated with the overall thermotropic transition (approximately 6 kcal/mol) is associated with this part of the transition. While the lower temperature limit of the main transition increases by only 1–2 °C with decreasing lipid concentration, the upper temperature limit of the transition increases to approximately 28 °C with decreasing lipid concentration.

The addition of cytochrome c promotes dramatic changes in the heat capacity curves of the DMPG dispersions (Figure 2). Note that the scale of the ordinate in Figure 2 is about a factor of 10 different from that in Figure 1. At all lipid concentrations, addition of excess protein results in a broadening of the phase transition with the C_p curve exhibiting essentially no structure and a single maximum at about 29 °C. Although the pure lipid phase behavior is quite different at 150 and 10 mM lipid concentrations, the heating scans in the presence of protein are similar. The enthalpy change
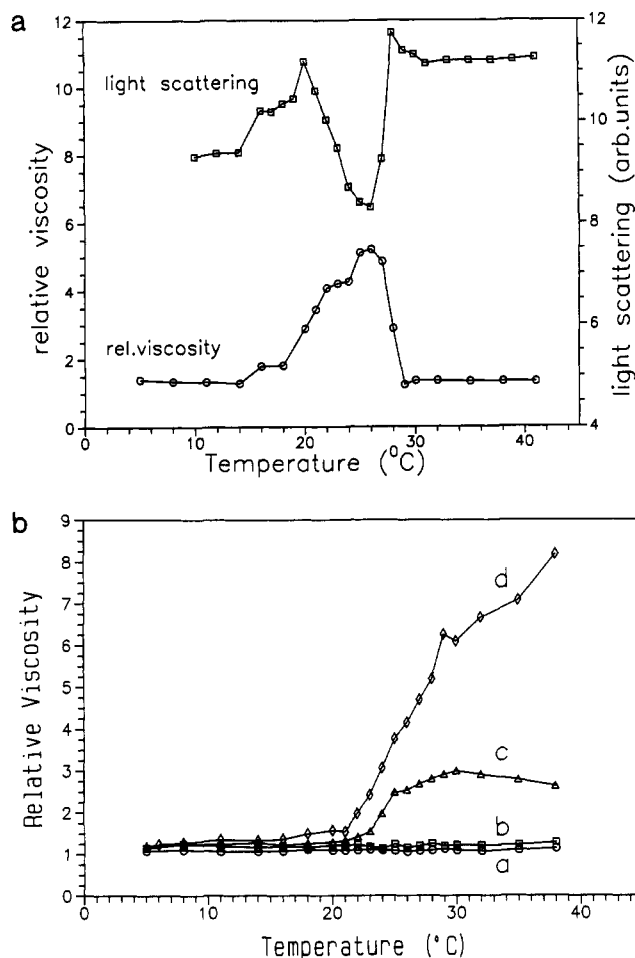

FIGURE 3: (a) Viscosity of a 13 mM DMPG dispersion relative to the viscosity of water as a function of temperature: 90° light scattering of a 13 mM DMPG dispersion at a wavelength of 280 nm as a function of temperature in 2 mM phosphate buffer and 1 mM EDTA, pH 7.5. (b) Viscosity of 13 mM DMPG dispersions in the presence of cytochrome c relative to the viscosity of water as a function of temperature: (curve a) 0.325 mM protein, (curve b) 0.65 mM protein, (curve c) 0.975 mM protein, and (curve d) 1.3 mM protein, corresponding to 25%, 50%, 75%, and 100% surface saturation with cytochrome c in 2 mM phosphate buffer and 1 mM EDTA, pH 7.5.

associated with this transition is protein concentration dependent, reaching a limiting value of 1.7 kcal/mol at a protein to lipid mole ratio of 1:10. At this mole ratio the lipid surface is thought to be saturated with protein (Görrissen et al., 1986).

Viscosity and Light-Scattering Measurements. Flow times of 13 mM DMPG in 2 mM phosphate buffer were measured over a temperature range of 5–40 °C using a Cannon viscometer and compared to the flow times of distilled water to yield relative viscosities (Figure 3a). At temperatures below and above the main thermotropic phase transition region, T < 20 and T > 28 °C, the viscosities of all dispersions are similar to that of water. The relative viscosity of the lipid dispersion begins to increase at approximately 20 °C, reaches a maximum at about 26 °C, and then decreases abruptly to the water value in a temperature range of about 1 °C.

In the low-viscosity states of the lipid below and above the main thermotropic phase transition region the solution appears milky. However, the light scattering decreased about 2-fold in the region where the viscosity of the lipid dispersion was maximal. This optical effect can be monitored by measurement of the light scattering at a wavelength of 280 nm, shown in Figure 3a. The anomalous thermal behavior of the heat
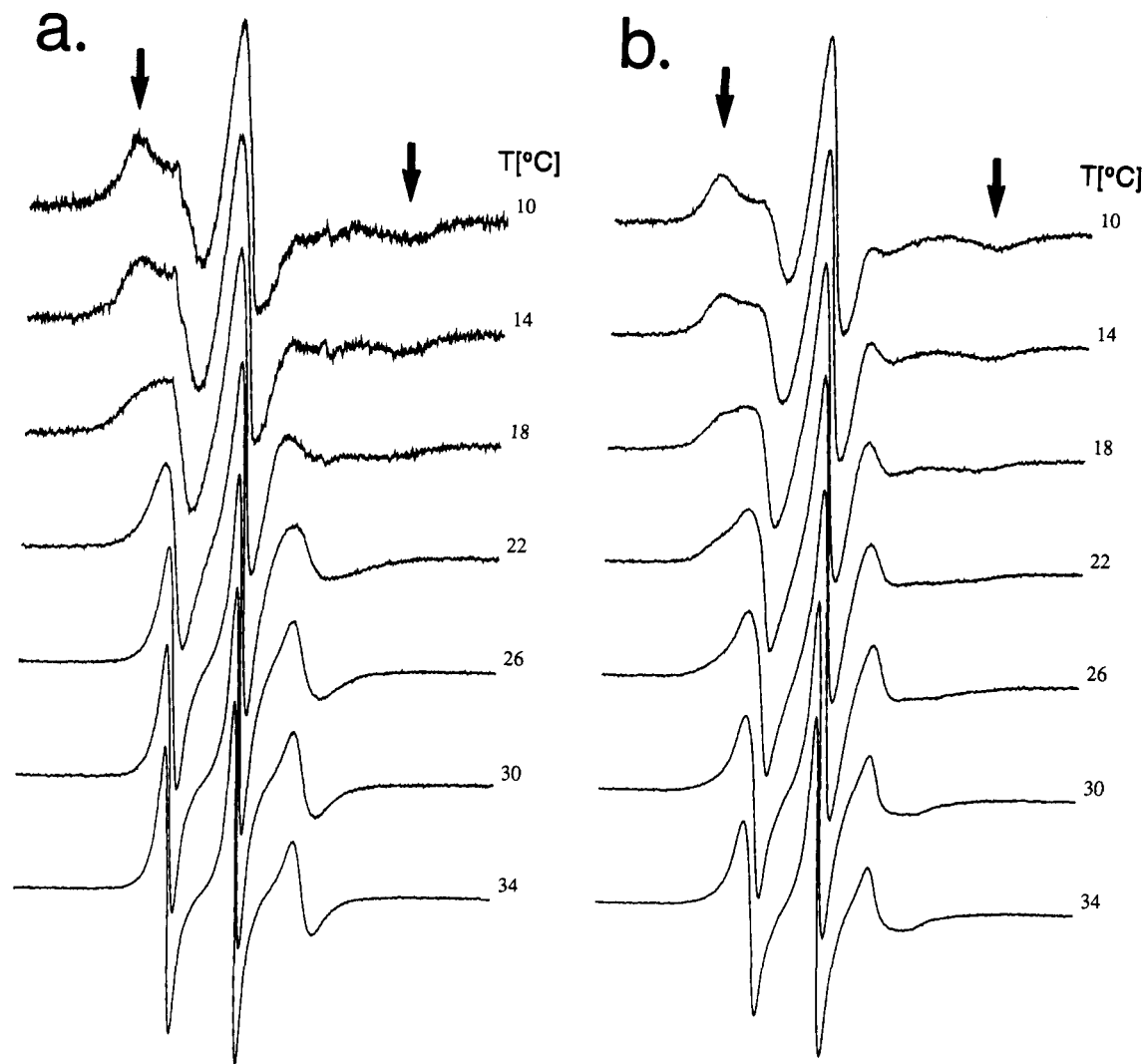
FIGURE 4: ESR spectra of (a) 45 mM DMPG and (b) complexes of 45 mM DMPG and 4.5 mM cytochrome *c*. Experiments were performed in 2 mM HEPES buffer and 1 mM EDTA at pH 7.5.

capacity, the viscosity, and the light scattering of the DMPG dispersion are all in correspondence on the temperature scale.

The relative viscosities of a 13 mM lipid dispersion in the presence 325 μM, 650 μM, 975 μM, and 1.3 mM cytochrome *c* are shown in Figure 3b. At protein–lipid ratios less than 1:20, no temperature anomalies of the viscosity were observed; the relative viscosity was essentially independent of lipid concentration. Upon further addition of protein the relative viscosity as a function of temperature changes. At a temperature of about 20 °C the viscosity begins to increase significantly. This temperature corresponds to the low-temperature limit of the transition in the presence of protein (Figure 2). At temperatures from 20 to 40 °C the sample remained in a viscous state. At a protein–lipid ratio of 1:10, the viscosity changes up to 8-fold compared to that of pure water. These viscosity changes are reversible upon cooling to 20 °C or less.

Magnetic Resonance Experiments. Further information about the physical state of DMPG and of the cytochrome *c*–DMPG complexes as a function of temperature was obtained by ESR and ^{31}P NMR experiments. Phosphatidylglycerol was labeled with a nitroxide at the 14th carbon of the *sn*-2 chain to obtain information about the configurational mobility of the lipid hydrocarbon chains as a function of temperature. Figure 4 shows the ESR spectra of 45 mM DMPG dispersions (panel a) and of complexes of DMPG and cytochrome *c* (45

mM lipid, 4.5 mM protein) (panel b) at several temperatures. The ESR spectra of the gel and the fluid lipid phases are distinguished by different degrees of motional averaging of the spectral anisotropy as monitored by the outer hyperfine splittings (see arrows in Figure 4). In pure DMPG dispersions (Figure 4a) a spectrum typical for gel-phase lipids is seen in the temperature range between 10 and 18 °C. A change in the spectra indicative of chain melting is also observed in the temperature range 18–26 °C. Above 26 °C the ESR spectra are indicative of fluid lipid phases. In the lipid–protein dispersion spectra (Figure 4b) a broad transition from a gel-state phase to a fluid phase can be observed between about 18 and 30 °C. The spectra in this interval suggest the coexistence of two lipid states with different degrees of motional freedom.

The results of the ESR experiments in Figure 4 are summarized quantitatively in Figures 5 and 6. The outer splittings of the ESR spectra in the absence (●) and in the presence of a saturating amount of protein (O) as a function of temperature are shown in Figure 5. The outer splittings are a function of the chain mobility at the C-14 position of the hydrocarbon chains, close to the center of the membrane. Major changes in the magnitude of the outer splitting are associated with the low-temperature end of the main transition (18–20 °C). If, however, line-height ratios are plotted as a function of temperature (Figure 6), significant chain
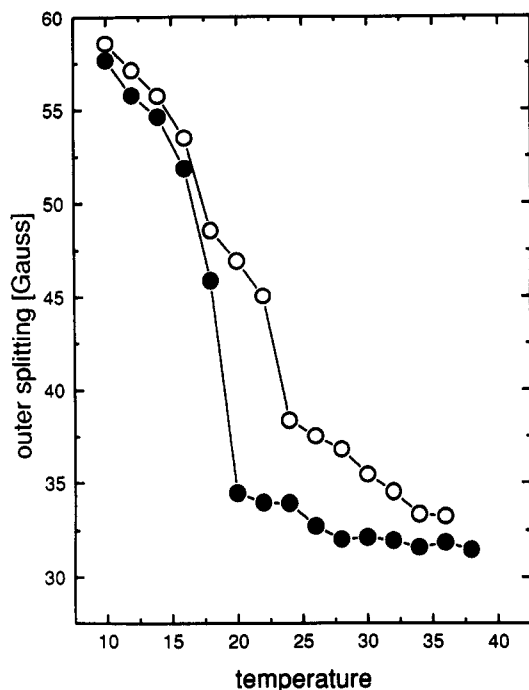
FIGURE 5: Outer hyperfine splitting of 45 mM DMPG (●) and of complexes of 45 mM DMPG and 4.5 mM cytochrome *c* (O) determined from the ESR spectra of Figure 4 as a function of temperature. The decrease in the outer splitting is indicative of lipid chain melting.
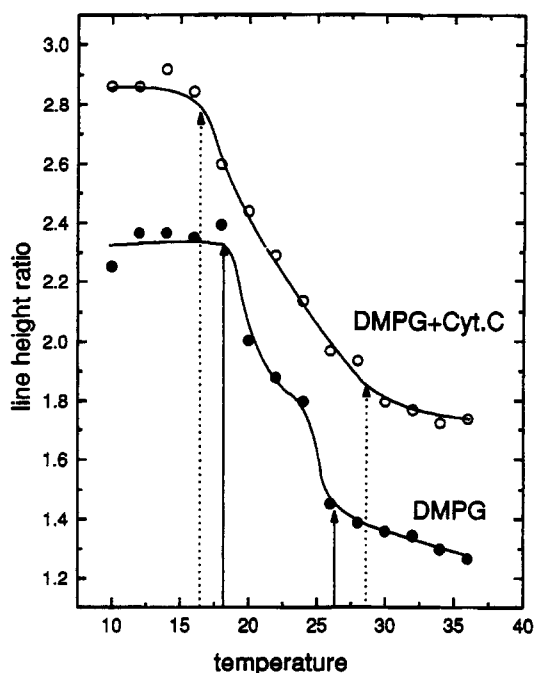

FIGURE 6: Line-height ratio derived from the ESR spectra shown in Figure 4 as a function of temperature: (a) 45 mM DMPG and (b) complexes of 45 mM DMPG and 4.5 mM cytochrome *c*. The line-height ratio is defined as C_2/C_1, where C_2 is the height of the central peak (2nd maximum - 2nd minimum) and C_1 is the height of the left-most peak (1st maximum - 1st minimum).

melting is observed in the main transition range in the absence of protein. In the presence of protein, the ESR spectra indicate a broad chain-melting transition with no apparent detail. These data are consistent with the heat capacity results shown in Figures 1 and 2 for the pure lipid and the lipid–protein complex, respectively.

Information about the morphological state of the lipids was obtained from ^{31}P NMR experiments. Figure 7 shows the

broad-band proton dipolar-decoupled spectra of 45 mM DMPG dispersions (panel a) and 45 mM DMPG/4.5 mM cytochrome *c* complexes (panel b) at three temperatures, below, within, and above the main chain-melting transition region described by the calorimetric and the ESR experiments. The NMR spectra of the pure lipid dispersion exhibit line shapes typical for lamellar phospholipid phases at all three temperatures. The chemical shift anisotropies of about 70 ppm at 11 °C and about 48 ppm at 35 °C are indicative of gel and fluid phase, respectively. In the presence of cytochrome *c* the spectra at all three temperatures are isotropic, with half-widths of ~2.2 ppm at 11 °C and ~1.4 ppm at 35 °C. This spectral shape does not allow identification of the exact nature of the phase. Isotropic peaks in ^{31}P NMR can be the result of several effects: (1) a local distortion of the membrane structure caused by proteins in a binding site; (2) an effect of the protein on head group orientation; (3) formation of small particles such as small vesicles and micelles; or (4) development of structures with high degrees of curvature such as those found in cubic phases.

It is difficult to distinguish the structural possibilities from the NMR spectra of the lipid–protein complexes. However, as shown by the ESR measurements at low temperatures, a gel phase is present which suggests the existence of a lamellar phase because, usually, nonlamellar lipid phases are observed only in the liquid crystalline state. Therefore, it is likely that the lipid exists in a lamellar form at low temperature. For the fluid-phase lipid–protein complexes, no such statement can be made. Neither the calorimetric nor the NMR data provide explicit information about the three-dimensional organization of the lipid under these conditions.

Negative Stain Electron Microscopy. Information about the morphology of the lipid and lipid–protein complexes was also obtained from negative stain electron microscopy studies. Samples were prepared at different temperatures in the presence and the absence of surface-saturating concentrations of cytochrome *c*. The dispersions were brought into contact with a carbon film and then stained with uranyl formate. Negative stains of the pure DMPG dispersion at 15, 24.5, and 35 °C, representing temperatures below, within, and above the main transition range of the lipid defined by the calorimetry and viscosity measurements, are shown in Figure 8a–d. All four micrographs show interconnected sheets or tubes of lipid. At 15 °C the structure appears to be breaking down and forming disc-like particles (Figure 8a). At 24.5 °C the network of tubes is pronounced (Figure 8b). At 35 °C the tubular rods become very long (Figure 8c). In some parts of the sample, breaking of these extended structures into vesicles of 20–50-nm diameter can be observed (Figure 8d).

In the presence of a saturating amount of cytochrome c (lipid–protein ratio 10:1, mole:mole) clear changes of the vesicular structures can be seen in the electron micrographs. At 15 °C 10–20-nm-diameter spheres form without any apparent intervesicular contact (Figure 8e). At 35 °C these vesicles appear to collapse into discs of about the same diameter and begin to make vesicle–vesicle contact by forming stacks of discs (Figure 8f). These results indicate that both in the absence and in the presence of cytochrome *c* there is a tendency of the lipid dispersions to form extended structures in the main transition region. The structures in the presence of cytochrome *c* appear to be quite different from those seen in the absence of protein.

Titration Calorimetry. The thermodynamics of the binding of cytochrome *c* to DMPG was investigated by titration microcalorimetry at a variety of temperatures. With each
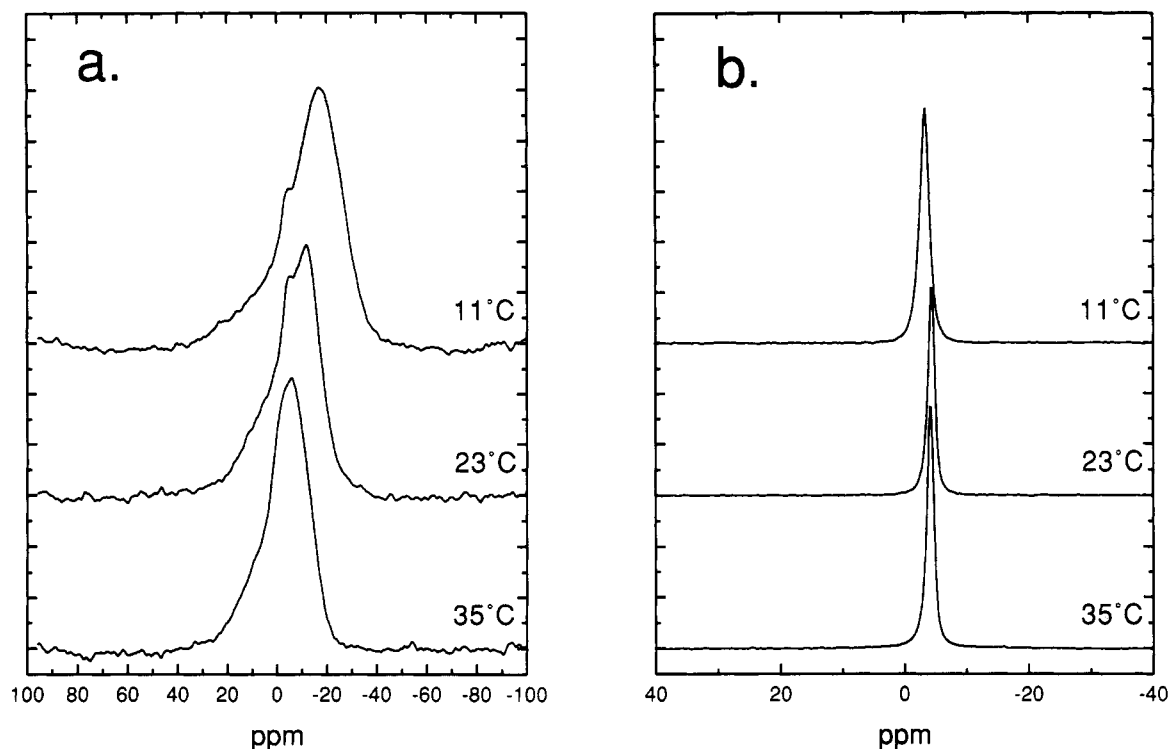
FIGURE 7: Proton dipolar-decoupled ^{31}P NMR spectra of (a) 45 mM DMPG, showing lamellar arrangement of lipids, and (b) complexes of 45 mM DMPG and 4.5 mM cytochrome *c*, showing an isotropic signal. Experiments were performed in 2 mM HEPES buffer and 1 mM EDTA at pH 7.5.

injection of protein, the heat release or the heat absorption was recorded. Experiments were performed in three buffer systems (TRIS, HEPES, and phosphate) to ascertain the net change in protonation upon interaction between the protein and the lipid (Flogel & Biltonen, 1975). The difference between the calorimetrically measured heats for any pair of buffers is $\delta\Delta H = \Delta n_H(\Delta H_1 - \Delta H_2)$ where ΔH_1 and ΔH_2 are the heats of protonation of two buffers and Δn_H is the net change in protonation upon complex formation. For all three pairs $\delta\Delta H$ was zero within experimental error. Since $\Delta H_1 \neq \Delta H_2$ for all three pairs, $\Delta n_H = 0$. All titration experiments described herein were done in 2 mM TRIS buffer, pH 7.5 (at room temperature), with 1 mM EDTA. Because of the significant enthalpy change associated with ionization of this buffer, the actual pH of the solutions was 7.5 ± 0.4 over the temperature range of this study. However, this variation in pH should have little effect on the results because zero net proton release or absorption occurs upon interaction of the protein and lipid. The experiments at 7, 22.6, and 41 °C shown in Figure 9 are examples of the three general types of isotherms obtained.

At 7 °C the first injection resulted in a rapid absorption of heat. The observed time dependence of this response is similar to the response time of the calorimeter. The heat measured with each injection became larger, and the time course of the calorimetric response became much slower, suggesting a slow process subsequent to initial formation of a lipid–protein complex at higher surface saturation. This biphasic kinetics of the binding reaction suggests that the protein is binding to two different states of the lipid, or that the lipid–protein complex is undergoing a change of state subsequent to binding.

At 19.8 °C the first injection produced two resolvable heat peaks, the first occurring within the response time regime of the calorimeter and the second being significantly slower (~3 min). The heats of reaction per injection decrease with increasing protein concentration. The slow process becomes

evident at lower protein–lipid ratios as the temperature is increased from 7 to 20 °C. Above 23 °C no slow reaction was observed. However, another process appears at these temperatures as can be seen in the 41 °C experiment (Figure 9c). At this temperature the calorimetric response at all protein concentrations was rapid, but the sign of the heat changes with protein concentration. This is another clear indication of the biphasic behavior of the binding process.

At temperatures below 23 °C heat is absorbed upon binding at all protein concentrations. At the lowest temperature, the shapes of the enthalpy binding isotherms (as in Figure 11) indicate clearly that protein binding is a cooperative process. At intermediate temperatures (19–22 °C), the integrated binding curves appear to be qualitatively consistent with a simple binding process. However, some anomalous behavior is observed in the details of the binding isotherm. At temperatures above 23 °C, the sign of the incremental reaction heat changes from endothermic to exothermic as protein concentration is increased. This is a clear indication that a second process is occurring upon, or subsequent to, the formation of the initial lipid–protein complex. At all temperatures, binding appears to be complete at a lipid–protein ratio in the range of 9:1 to 10:1 except at 7.0 °C where it was found to saturate at a mole ratio of 7:1. These results are consistent with the reported stoichiometry of 9:1 (Görrissen et al., 1986).

The total heat change upon addition of an excess of cytochrome *c* varies from 7 kcal/mol of lipid at low temperature to about 3 kcal/mol of lipid at high temperatures (Figure 10). These values correspond to 70 and 30 kcal/mol of protein, respectively, assuming a 10:1 stoichiometry. This difference of 4 kcal/mol of lipid is similar to the difference of the total enthalpy change (4.3 kcal/mol) for the lipid transition obtained with DSC in the absence and the presence of saturating protein.
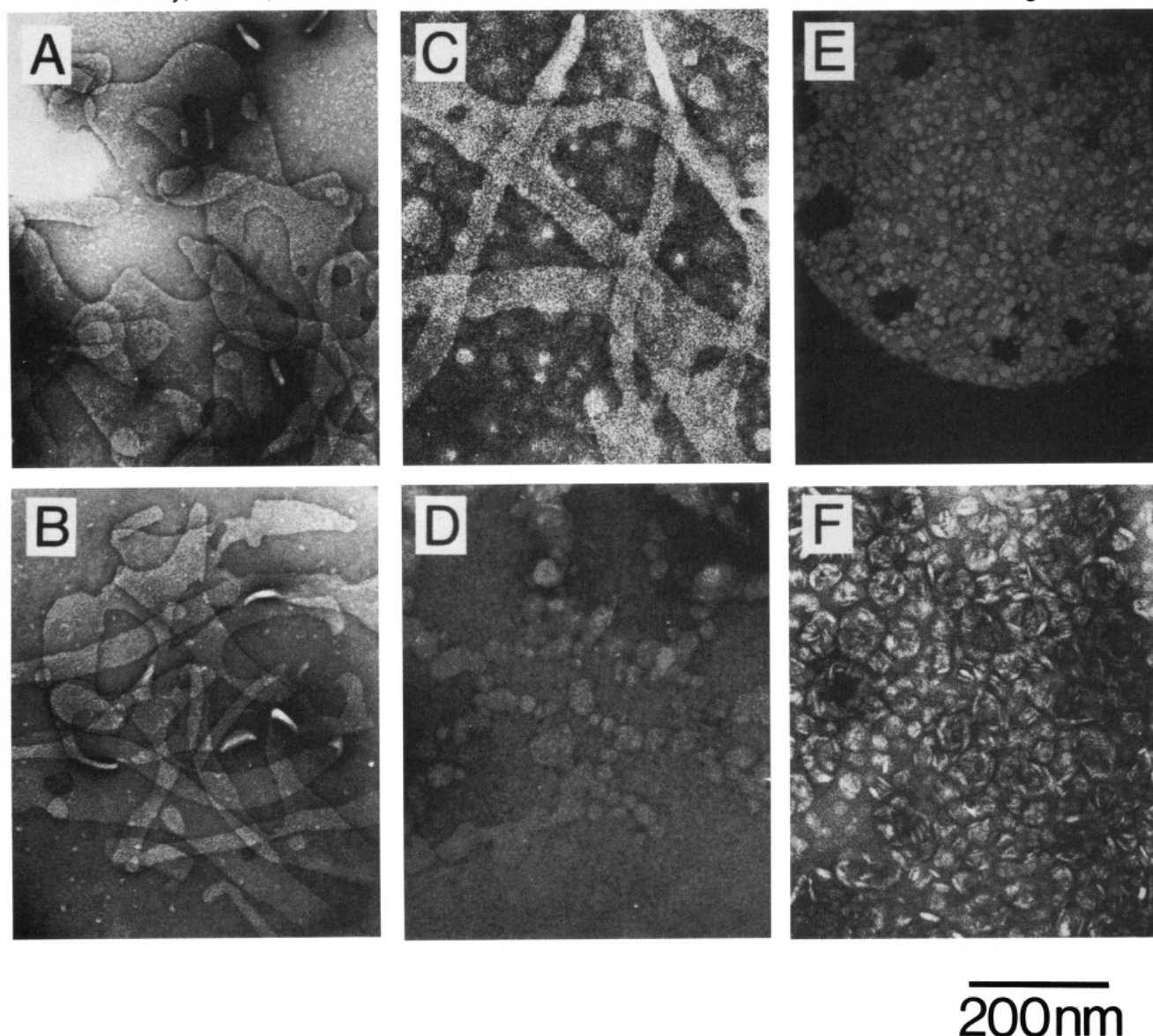
200nm

FIGURE 8: Negative stain electron micrographs of lipid dispersions in 2 mM HEPES buffer (1 mM EDTA, pH 7.5): (a) 10 mM DMPG at 15 °C, (b) 200 μM DMPG at 24.5 °C, (c) 10 mM DMPG at 35 °C, (d) 10 mM DMPG at 35 °C, (e) 10 mM DMPG at 15 °C in the presence of excess cytochrome c, and (f) 10 mM DMPG at 35 °C in the presence of excess cytochrome c. Panels c and d are different fields of the same electron micrograph. The small white spots in panel c are artifacts produced by the negative stain procedure at high temperatures.

Table 1: Thermodynamic Parameters Used for Computer Simulations of Binding Data[a]

T (°C)	K_a (mol^{-1})[b]	K_b (mol^{-1})[b]	K_o[c]	$\Delta H_a/m$ (kcal/mol)[d]	$\Delta H_b/m$ (kcal/mol)[d]	m
7.0	2×10^6	3×10^6	2.4×10^{-4}	2.71	5.96	7
9.4	2×10^6	3×10^6	1.0×10^{-4}	3.56	7.78	9
12.8	5×10^5	7.5×10^5	1.0×10^{-3}	7.00	6.78	9
16.3	1×10^6	1.4×10^6	2.0×10^{-3}	4.78	5.56	9
19.8	1×10^6	1.27×10^6	6.0×10^{-2}	6.90	4.45	10
22.6	1×10^6	1.27×10^6	6.0×10^{-2}	7.60	2.95	10
25.1	2×10^6	2.59×10^6	3.0×10^{-2}	8.00	2.55	10
29.4	2×10^6	2.59×10^6	1.7×10^{-2}	9.0	2.43	10
34.9	1×10^6	1.35×10^6	5.7×10^{-3}	8.0	2.16	10
41.0	1×10^6	1.35×10^6	2.6×10^{-3}	9.2	2.48	10

[a] These values were obtained for $N = 25$. Definitions of parameters are given in the text. [b] Per mole of lipid binding site. [c] Per mole of cooperative binding unit. [d] Per mole of lipid.

The experimental calorimetric titration data have been analyzed using a statistical thermodynamic model assuming coupling between protein binding and lipid structural changes as described in the Materials and Methods section. Figure 11 shows computer simulations (—) of the binding data (O) at three different temperatures. Good fits were obtained; data at all other temperatures were simulated equally well using the parameters listed in Table 1. Because of the strong

statistical coupling between $\Delta H°$ and ΔH_b, $\Delta H°$ (the enthalpy change associated with the putative lipid structural change) was set to zero. That does not mean, however, that no heat is involved in the transition. The binding constants K_a and K_b differ from one another only slightly in all the simulations. Binding constants always were estimated to be between 5×10^5 and 5×10^6 1/mol of protein in both states. This is because we assumed N, the number of protein sites coupled coopera-
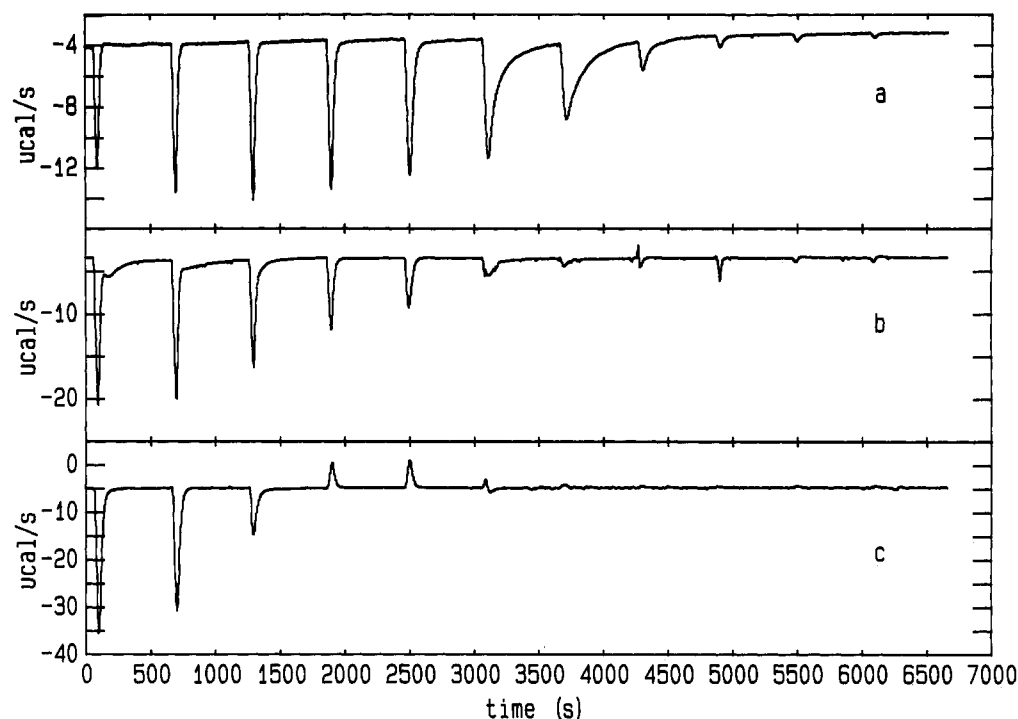
FIGURE 9: Calorimetric titration experiments at various temperatures: (a) 9.4 °C, (b) 22.6 °C, and (c) 41 °C. The heat release is plotted as a function of time. A cytochrome *c* solution (1.61 mM) was titrated into a lipid dispersion (0.536 mM DMPG). Both solutions were 2 mM TRIS buffer and 1 mM EDTA, pH 7.5, in the reaction cell. Each injection consisted of adding 10 μL of the protein solution to 1.4 mL of the lipid dispersion.
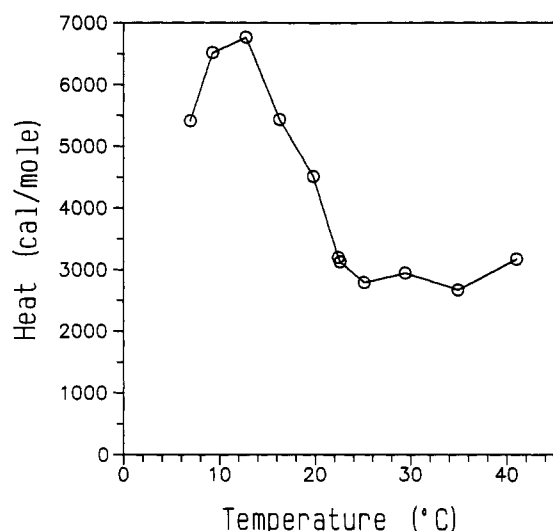

FIGURE 10: Integrated heats obtained from the data as in Figure 9 after correction for the heat of dilution of the protein as a function of temperature at saturation of the lipid surface with cytochrome *c*.
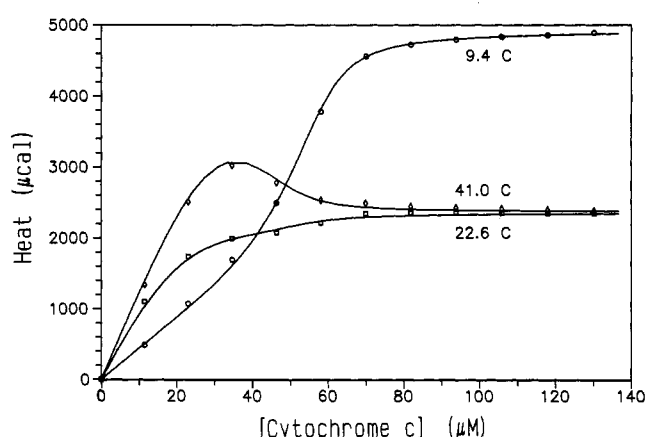

FIGURE 11: Computer simulations of the enthalpy titration curves at three different temperatures (9.4, 22.6, and 41 °C) using the statistical thermodynamic model described in the text and the parameters given in Table 1. Open symbols represent experimental data corrected for heats of dilution.

tively, to be 25. Since the thermodynamic condition to obtain cooperative binding is

$$\delta \Delta G^\circ = NRT \ln \frac{K_B}{K_A} > -RT \ln K_o$$

changing N would result in different values of K_a and K_B required to describe the data. The results of our simulations indicate that $\delta \Delta G^\circ$ varies from 3.1 to 5.8 kcal/mol and exceeds $-RT \ln K_o$ by 0.5–3.8 kcal/mol, depending on the temperature. This is sufficient to shift the lipid equilibrium from essentially all form A in the absence of protein to greater than 70% form B in the presence of saturating protein at all temperatures. This means literally that while the lipid structural change

does not alter protein affinity significantly, protein binding can alter greatly the lipid structural organization.

DISCUSSION

The thermotropic behavior of DMPG dispersions at low ionic strength is characterized by three distinct temperature regions according to the viscosity of the system. A region of low viscosity exists in the temperature range below 20 °C (Figure 3a). A region of very high viscosity exists at temperatures above 20 °C and extending to 28 °C depending upon the lipid concentration. We refer to this region as the main transition region. The third region is one of low viscosity existing at higher temperatures. ^{31}P NMR (Figure 7) indicates that the lipid exists in lamellar form throughout the temperature range of 11–35 °C. Electron microscopic studies indicate that the lipid phase(s) at 15 °C consists of a mixture

of moderately extended particles and disc-shaped vesicles of about 50-nm diameter (Figure 8a). At 35 °C, well above the main transition region, the system appears to consist of elongated extended structures (Figure 8c,d) with regions of associated, smaller particles. Only at 24.5 °C do extended lipid structures dominate the microscopic field (Figure 8b). The electron microscopic results demonstrate quite clearly that extended structures of DMPG exist even at low concentration. Furthermore, the extended structures do not appear to be limited to the optically isotropic, highly viscous phase region.

DSC experiments (Figure 1) indicate a single thermotropic transition in the lowest temperature region, whereas no anomolous behavior is observed in the highest temperature region. However, a sequence of thermotropic transitions is observed in the main transition region. The details of the transitions are both lipid concentration and scan rate dependent. At constant scan rate, the position and value of the C_p maximum at 15 °C increase with decreasing lipid concentration, although the small enthalpy change remains constant ($\Delta H = 0.57 \pm 0.14$ kcal/mol); at constant lipid concentration, the temperature position and heat capacity maximum increase with increasing scan rate. These latter properties are not due to the time response of the calorimeter and indicate that the transition is kinetically slow. This latter characteristic (Lentz et al., 1978), along with the small ΔH and the absence of significant light scattering or viscosity change, suggests that the transition may be due to the formation of a P_{β}' (ripple) phase, although no direct physical evidence exists to support this conjecture. In the temperature range of 20–28 °C, a complex, lipid-concentration-dependent C_p profile is observed. It is characterized at low lipid concentration by two well-defined maxima at the high- and low-temperature edges of the main transition, which correlate with the temperature-dependent changes in the line-height ratio of the ESR signal (Figure 6). The heat capacity does not return to "baseline" values in the temperature range between these two maxima, and there is some indication of a fourth C_p maximum. Increasing lipid concentration induces coalescence of the two primary C_p maxima; at 150 mM lipid the C_p profile is best described as a single maximum with a high-temperature shoulder.

A more detailed evaluation of the DSC data provides some further insight into the possible nature of the main transition. First, the total enthalpy change of the lipid transitions (6 kcal/mol), calculated by integration of the excess heat capacity function from 9 to 30 °C, is independent of lipid concentration within experimental error. This means that the complete set of transitions the lipid undergoes is energically identical at all lipid concentrations. Second, the position of the heat capacity maximum at 22 ± 1 °C is only slightly dependent on lipid concentration. At low lipid concentration this transition is quite well resolved with an estimated $\Delta H = 0.38 \pm 0.17$ kcal/mol. This C_p maximum becomes quite large at slow scan rates, an indication that the transition is extremely cooperative. The width at half-height of the C_p is 0.3 °C, which is approaching that observed for the chain-melting transition of multilamellar dipalmitoylphosphatidylcholine ($\Delta T_{1/2} = 0.07$ °C) (Biltonen, 1990; Albon & Sturtevant, 1978). Third, at high lipid concentrations a single, sharp transition at about 22 °C is no longer obvious, although the position of the first C_p maximum does not change significantly. Assuming that the sequence of these transitions is identical at all lipid concentrations, this observation suggests that the transition

at 22 °C is coupled to subsequent thermally induced changes that are lipid concentration dependent.

The well-resolved heat capacity maximum at the high-temperature end of the complex transition varies from 23 °C at high lipid concentration to about 28 °C at low lipid concentration. Assuming that all C_p data represent, or at least closely approximate, equilibrium, this result would indicate that the high-temperature state is more aggregated than the intermediate state. However, electron micrographs obtained at 24.5 °C indicate that the intermediate state (that which exists in the main transition region) is apparently the more extended or aggregated state. Furthermore, the dramatic, essentially concomitant increase in viscosity and decrease in light scattering indicate that this intermediate phase consists of an extended lipid structure rather than an aggregation of basic lipid particles (e.g., vesicles). If this is true, then the lipid concentration dependence of the high-temperature transition could reflect a difference in the degree of hydration of the two states and that hydration of the intermediate state must be less than complete under these low ionic strength conditions. Gershfeld et al. (1986) suggested that the highly viscous state of DMPG was a structure with long-range order. To the best of our knowledge, this is the first experimental report of an optically isotropic, viscous state persisting at even very high degrees of hydration in phospholipids. The exact structural nature of this phase remains to be determined, but in the absence of protein it is probably lamellar and may be analogous to the L_3 type phase reported by Strey et al. (1990) for surfactant–water systems. Strey et al. (1990) describe the L_3 phase to be a bicontinuous bilayer network with very high water content. In contrast to cubic lipid phases, no regular structural arrangement is seen in the L_3 phase.

The presence of cytochrome c alters the thermotropic phase behavior of DMPG significantly (Figure 2). The C_p profile loses its detail with only a single C_p maximum observed. The total enthalpy change obtained by integration of C_p is reduced from about 6 kcal/mol in the absence of protein to 1.7 kcal/mol under saturating conditions, and the temperature position and range of the main transition region are both increased in the presence of protein. Partial (25–50%) saturation of the lipid with protein eliminated any temperature-dependent increase in the viscosity (Figure 3b). At 75–100% saturation, a temperature-dependent increase in viscosity is observed with a high-viscosity state being maintained at high temperature.

The ^{31}P NMR spectra in the presence of protein are isotropic, leaving open the question of the lipid structure under such conditions. However, electron micrographs of DMPG dispersions in the presence of excess protein at 15 °C (Figure 8e) suggest an array of small particles; at 35 °C electron microscopy (Figure 8c) suggests the existence of highly curved vesicular structures in an aggregated state. Such aggregated, highly curved lipid–protein complexes are consistent with the isotropic ^{31}P NMR spectra and the persistence of a high viscosity at elevated temperature in the presence of excess enzyme.

It is clear that DMPG exists as several different structures over a broad temperature range and that the presence of protein alters the equilibrium poise of the system. The form of the calorimetric binding data (Figures 9 and 11) indicates that protein–lipid association is a complex process coupled to lipid structural changes as described above. All of the calorimetric binding curves can be analyzed in terms of a relatively simple model consisting of a conjugated set of protein binding sites as described in the Materials and Methods section. The

analysis was performed at each temperature independently; no attempt at a global statistical analysis was made. Nevertheless, the results from this analysis demonstrate two consistencies. Under all conditions, the net enthalpy change is positive and the binding is positively cooperative. It should be noted that the parameters are not unique and that the rationalization of the complex nature of the isotherms is totally in terms of the intrinsic ΔH of binding to specific lipid states. The binding to the two types of sites postulated is very tight and almost, but not exactly, equivalent. Regardless of the details of the model, cooperative binding of cytochrome *c* to DMPG must be invoked to rationalize the data, which we interpret to be the result of coupling between binding and the complex thermotropic behavior of the lipid. The degree of cooperativity is a reflection of the number of lipids linked in an almost all-or-nothing transition to protein binding. Ramsay et al. (1986) have reported similar calorimetric titration results for the interaction of myelin basic protein with phosphatidylserine vesicles and interpret their data in terms of a coupled binding reaction scheme.

The DSC and titration calorimetric results are thermodynamically self-consistent. That is, the sum of the transition enthalpy changes and the binding enthalpy at high temperature is equal to the binding enthalpy at low temperature plus the transition enthalpy measured in the presence of the protein. Since the apparent affinity does not change significantly with temperature, the measured heats of binding ($\sim$50–70 kcal/mol of protein) must primarily reflect the enthalpy changes associated with the protein-induced structural changes in the lipid. At low temperature, the ΔH° is probably associated with the lipid structural change associated with the lowest temperature transition. At high temperature, the enthalpy changes could be associated with aggregation of protein-bound vesicles. At intermediate temperatures, the interpretation is not as clear, although the enthalpy change reflects, at least in part, the disruption of the highly viscous and, presumably, isotropic lipid state.

These results complement previous studies on the binding of cytochrome *c* to lipid dispersions which demonstrated that cytochrome *c* in the lipid-bound state existed as an equilibrium of two conformational states, and that the position of this equilibrium was dependent upon the temperature-dependent structural state of the lipid. Similar shifts in the conformational equilibrium of the protein could be induced by the addition of relatively small amounts of dioleoylglycerol or dioleoylphosphatidylcholine to dioleoylphosphytidylglycerol. An isotropic component in the ^{31}P NMR spectra has also been observed in complexes of cytochrome *c* with liquid crystalline dioleoylphosphatidylglycerol (DOPG) (Heimburg et al., 1991) and was proportional to the amount of protein bound. It was argued that the isotropic component is likely caused by local disorder or curvature in the protein binding site of a planar surface rather than by changes in macroscopic lipid arrangement into nonlamellar lipid states. Those results and their interpretation are consistent with those of the current study. What we have shown, at least for DMPG in the liquid state, is that protein binding promotes a disruption in the long-range order of lamellar lipid and formation of aggregates of highly curved vesicule-like structures.

Whenever there is thermodynamic coupling of protein binding to a structural transition of a lipid surface, cooperative binding to the lipid will be observed. The implications of such a phenomenon are interesting and may be of some biological importance. In systems consisting of two lipid species (either structurally or chemically distinct), the binding of protein can promote the localization on the surface of that lipid species which the protein prefers thermodynamically (Heimburg & Biltonen, 1993). This localization of lipid can induce further binding and localization of the protein. From a topological perspective, it would appear that protein is aggregating on the membrane surface, although no specific interaction between proteins need be postulated. This argument can be extended to nonidentical proteins if they all prefer the same lipid or lipid structure.

The formation of lipid domains has been postulated for biological membranes [see, for example, Thompson et al. (1992)], although a clear demonstration that this is the case is lacking. However, the activity of both phospholipase A$_2$ (PLA2) and protein kinase C (PKC) can, in general, be modulated in a critical fashion by lipid composition. In the case of phospholipase A$_2$-catalyzed hydrolysis of phosphatidylcholine vesicles, the onset of high activity is temporally correlated with lateral phase separation of the reaction products (Burack et al., 1993) and the time required to achieve this type of activation is least near the gel–liquid crystalline transition temperature of the lipid substrate (Litchenberg et al., 1986). Although binding is a prerequisite for activity, experimental conditions can be established for both PKC (Orr & Newton, 1992) and PLA2 (Burack & Biltonen, 1994) where the enzyme is completely bound by the membrane, but activity is minimal. This would suggest that a specific structural feature of the membrane is required for activity. It has been suggested for both PLA2 and PKC that this structural feature is one in which the lipid resembles a hexagonal II phase (Damson et al., 1984; De Boeck & Zidovetzki, 1989, 1992; Epand, 1990) and that fluctuations in the structure are important (Sen et al., 1991; Biltonen, 1990). If this is true, then thermodynamic coupling between protein binding and dynamic membrane structure is an important aspect of function. This study with cytochrome *c* may be a prototypic example of such coupling.

REFERENCES

Albon, N., & Sturtevant, J. M. (1978) *Proc. Natl. Acad. Sci. U.S.A. 75*, 2258.

Bell, J. D., & Biltonen, R. L. (1989) *J. Biol. Chem. 264*, 225–230.

Biltonen, R. L. (1990) *J. Chem. Thermodyn. 22*, 1–19.

Burack, W. R., & Biltonen, R. L. (1994) *Chem. Phys. Lipids* (in press).

Burack, W. R., Yuan, Q., & Biltonen, R. L. (1993) *Biochemistry 32*, 583–589.

Comfurius, P., & Zwaal, R. F. A. (1977) *Biochim. Biophys. Acta 488*, 36–42.

Cortese, J. D., & Fleischer, S. (1987) *Biochemistry 26*, 5283–5293.

Damson, R. M. C., Irvine, R. F., Bray, J., & Quinn, P. J. (1984) *Biochem. Biophys. Res. Commun. 125*, 836–842.

De Boeck, H., & Zidovetzki, R. (1989) *Biochemistry 28*, 7439–7466.

De Boeck, H., & Zidovetzki, R. (1992) *Biochemistry 31*, 623–630.

De Kruijff, B., & Cullis, P. R. (1980) *Biochim. Biophys. Acta 602*, 477–490.

Epand, R. M. (1990) *Biochem. Cell Biol. 68*, 17–23.

Epand, R. M., & Lester, D. S. (1990) *Trends Pharmacol. Sci.* *11*, 317–320.

Flogel, M., & Biltonen, R. L. (1975) *Biochemistry 14*, 2610–2615.

Gershfeld, N. L. (1989) *Biochim. Biophys. Acta 988*, 335–350.

Gershfeld, N. L., Stevens, W. F., & Nossal, R. J. (1986) *Faraday Discuss. Chem. Soc.*, No. 81, 19–28.

Goldberg, E. M., Borchardt, D. B., & Zilovetzki, R. (1993) *Biophys. J. 64*, A66.

Gonias, S. L., Allietta, M., Pizza, S. V., Castellino, F. J., & Tilliack, T. W. (1988) *J. Biol. Chem. 263*, 10903–10906.

Görrissen, H., & Marsh, D. (1986) *Biochemistry 25*, 2904–2910.

Heimburg, T., & Biltonen, R. (1993) 11th International Biophysics Congress, Budapest, Hungary, C5.25 (abstr.).

Heimburg, T., Hildebrandt, P., & Marsh, D. (1991) *Biochemistry 30*, 9084–9089.

Hildebrandt, P., & Stockburger, M. (1989a) *Biochemistry 28*, 6710–6721.

Hildebrandt, P., & Stockburger, M. (1989b) *Biochemistry 28*, 6722–6728.

Hildebrandt, P., Heimburg, T., & Marsh, D. (1990) *Eur. Biophys. J. 18*, 193–201.

Jain, M. K., & Berg, O. G. (1989) *Biochim. Biophys. Acta 1002*, 127–156.

Lentz, B., Freire, E., & Biltonen, R. L. (1978) *Biochemistry 17*, 4475.

Lindblom, G., & Rilfors, L. (1989) *Biochim. Biophys. Acta 988*, 221–256.

Mariani, P., Luzzati, V., & Delacroix, H. (1988) *J. Mol. Biol. 204*, 165–189.

Marsh, D., & Watts, A. (1982) *Lipid–Protein Interact. 2*, 53–126.

Monod, J., Wyman, J., & Changeux, J.-P. (1965) *J. Mol. Biol. 12*, 88–118.

Nishizuka, Y. (1984) *Nature 308*, 693–698.

Nishizuka, Y. (1986) *Science 233*, 305–311.

Orr, J. W., & Newton, A. (1992) *Biochemistry 31*, 4661–4667.

Ramsay, G., Prabhu, R., & Freire, E. (1986) *Biochemistry 25*, 2265–2270.

Seddon, J. M., Cevc, G., Kay, R. D., & Marsh, D. (1984) *Biochemistry 23*, 2634–2644.

Sen, A. T., Isa, V., & Hui, S.-W. (1991) *Biochemistry 30*, 4516–4521.

Sporetto, M. M., & Mouritsen, O. G. (1991) *Eur. Biophys. J. 19*, 157–168.

Strey, R., Jahn, W., Porte, G., & Basserea, P. (1990) *Langmuir 6*, 1635–1639.

Surewicz, W. K., Moscarello, M. A., & Mantsch, H. H. (1987) *Biochemistry 26*, 3881–3886.

Suurkuusk, Y., Lentz, B., Barenholz, Y., Biltonen, R. L., & Thompson, T. E. (1976) *Biochemistry 15*, 1343.

Thompson, T. E., Sankaram, M. B., & Biltonen, R. L. (1992) *Comments Mol. Cell. Biophys. 8*, 1–15.

Wiseman, T., Williston, S., Brandts, J. F., & Lin, L.-N. (1989) *Anal. Biochem. 179*, 131–137.

Wyman, J., & Gill, S. J. (1991) *Binding and Linkage*, University Science Books, Mill Valley, CA.

Zidovetzki, R., Laptalo, L., & Crawford, J. (1992) *Biochemistry 31*, 7683–7691.